ACI STRUCTURAL JOURNAL TECHNICAL PAPER

Title No. 114-S73

Reinforced Concrete One-Way Slabs with Large Steps

by Thomas H.-K. Kang, Sanghee Kim, Seongwon Hong, Geon-Ho Hong, and Hong-Gun Park

To evaluate the performance of relatively large steps in reinforced concrete one-way slabs in terms of the flexural behavior of the stepped slabs, a total of 12 specimens with various shapes of steps and different reinforcing details in steps were tested. The primary purpose of this research is to investigate the structural behavior of one-way slabs with steps and to evaluate the performance of steps in slab depending on various details. In comparing the conventional one-way slab with the stepped slab, it was found that: 1) the specimen without supplementary reinforcement in the step showed a very low moment strength and significant damage; 2) the specimens with diagonal reinforcement in the step exhibited substantial early cracks, experienced hinging of the step, and demonstrated a substantial loss of moment strength; and 3) the specimens with a combination of U-bars, inverted U-bars, L-bars, and inverted L-bars performed very well, reaching almost 100% of moment strength of the one-way slab. The U-bars and inverted U-bars were effective in controlling the diagonal cracks, while the L-bars and inverted L-bars were effective in preventing yielding of the slab reinforcement near the step. Based on the crack pattern and the analysis of the structural performance, the design guidelines of reinforcement details of stepped slabs were proposed.

Keywords: crack pattern; moment strength; one-way slab; step; structural performance; supplementary reinforcement.

INTRODUCTION

In recent times, building owners (or architects) have started to ask architects (or themselves) and engineers to design flexible space and different height of the floor elevation because of the aesthetic purpose or the functional purpose of mechanical equipment and ductwork (Moehle 1996; Hueste and Wight 1999; Robertson et al. 2002; Kang and Wallace 2005; Han et al. 2006; Kang et al. 2009; Rha et al. 2014; Lee et al. 2016). Use of step in a beam or slab is considered as a potential solution for the owners' recent requirements. In June 2012, the American Concrete Institute published an article titled "Steps in Beams" as a Detailing Corner feature in *Concrete International* (American Concrete Institute 2012). The ideal location of steps in members and reinforcement details in step are still controversial. In the article, several reinforcement details were proposed for three situations. The first case was for top steps in beams, which has also three subcases: 1) a subcase where the step is 75 mm (3 in.) or less; 2) a subcase where step exceeds 75 mm (3 in.); and 3) a subcase where step is located adjacent to a column or a transverse beam (Fig. 1). The second and third cases were for bottom and large steps, respectively. Although the article indicated that demands for appropriate reinforcement details of steps in beams or slabs are gradually rising due to elevated flooring and installed mechanical equipment or ductwork, limited experimental research and reports exist. To the authors' knowledge, there is no available literature related to slab, which is one of the most popular structural elements and frequently used for the ground and elevated floors of buildings. To bridge this gap, this study conducts full-scale experiments of a variety of features related to one-way slabs with step and suggests alternate options on how to place reinforcement in steps based on the observation and test data. The reinforcement detailing for staircase steps attached to the wall is different from that for one-way members under high shear and moment.

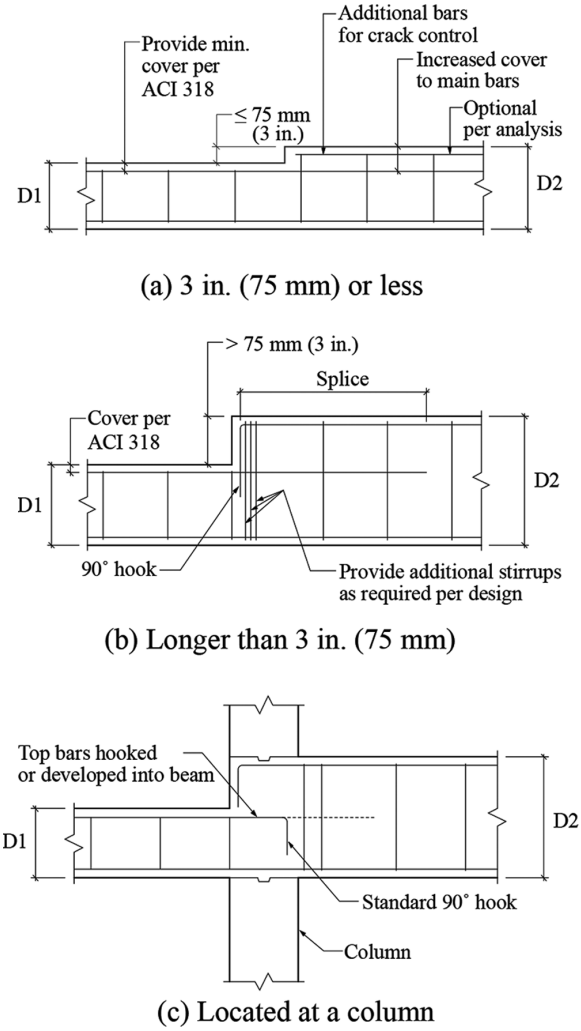

Fig. 1—Three subconditions of steps (redrawn from American Concrete Institute [2012]).

The main objective of the full-scale experiments is to investigate the structural performance of reinforced concrete

ACI Structural Journal, V. 114, No. 4, July-August 2017.
MS No. S-2016-147.R1, doi: 10.14359/51689459, was received April 12, 2016, and reviewed under Institute publication policies.

Table 1—Design configurations of slabs

Specimens	f'_{c_meas}, MPa	f_{y_meas}, MPa	Height of step, mm	Length of lower slab, mm	Thickness of step, mm	Supplementary reinforcement	Termination of slab bars in step
CTRL	28.0	588	—	—	—	—	Straight
N-210-HK	23.9	588	230	1090	210	None	135-degree hook
N-250-HK	23.9	588	230	1090	250	None	135-degree hook
IU-210-SLP	21.2	569	230	1090	210 + 180 (slope)	IU	Straight
IU-400	23.5	569	230	1090	400	IU	Straight
A-210-HK	28.0	588	230	1090	210	Type A	135-degree hook
A-IU-210-HK	29.8	588	230	1090	210	Type A+IU	135-degree hook
A-IU-210	23.1	569	230	1090	210	Type A+IU	Straight
B-IU-210-HK	29.8	588	230	1090	210	Type B+IU	135-degree hook
C-210-HK	30.0	588	230	1090	210	Type C	135-degree hook
C-210	23.1	569	230	1090	210	Type C	Straight
C-210-LLS	23.5	569	230	2700	210	Type C	Straight

Notes: CTRL is control specimen (one-way slab without step); N is no supplementary reinforcement; HK is 135-degree hook termination; IU is inverted U-bars; SLP is sloped step; LLS is long lower slab; f'_{c_meas} is measured concrete compressive strength at test day; f_{y_meas} is measured yield strength of slab reinforcement; 1 MPa = 0.145 ksi; 1 mm = 0.0394 in.

one-way slabs with large steps in terms of the flexural behavior of the stepped slabs. The slabs with different thickness (210 to 400 mm [8.3 to 15.8 in.]), length (1090 to 2700 mm [42.9 to 106.3 in.]), and slope of steps were tested to examine the influence of step shape and size. Moreover, with the use of three types of supplementary reinforcement, it is possible to evaluate the effects of additional reinforcement on the performance of one-way slabs with steps. Based on the pattern of cracks and the analysis of the structural performance, reinforcement details of stepped slabs can be developed.

RESEARCH SIGNIFICANCE

In *Concrete International*'s "Detailing Corner: Steps in Beams" (American Concrete Institute 2012), steps in beams and the modification of reinforcement details in steps were briefly discussed and suggested. Although there are potential demands for steps in beams and slabs of building systems, little information is available regarding the steps in beams and slabs. More specifically, based on the authors' knowledge, no large-scale experimental studies have been performed on reinforced concrete one-way slabs with large steps, which are features widely used in actual construction sites. The analysis of test results and design proposal of reinforcement details in stepped slabs can be employed to contribute to the work of Joint ACI-CRSI Committee 315, Details of Concrete Reinforcement.

EXPERIMENTAL PROGRAM

Design of test specimens

A total of 12 units were built and tested. Test specimens of one-way slabs were designed in accordance with the Korean Building Code 2009 (Architectural Institute of Korea 2009). The one-way slab had dimensions of 1000 mm (39.4 in.) wide, 5800 mm (228.0 in.) long, and 210 mm (8.3 in.) thick. Detailed information about the 12 one-way slab with and without steps is summarized in Table 1. The SD500, D13 longitudinal bars (Grade 75 [No. 4] bars) were placed at the top and bottom of the slab at spacing of 150 mm (5.9 in.), and the reinforcement in the step was SD500 D13 bars (Grade 75 [No. 4] bars) arranged in various patterns, as shown in Fig. 2. The SD600 D16 bars (Grade 90 [No. 5] bars) were only employed for the diagonal reinforcement of A-IU-210. Three types of supplementary reinforcement—Types A, B, and C—were adopted in the test specimens, as depicted in Fig. 3(a), 3(b), and 3(c), respectively. The specified concrete compressive strength f'_c was 24 MPa (3.5 ksi).

The first round of experiments was carried out on seven test specimens: CTRL, N-210-HK, N-250-HK, A-IU-210-HK, A-210-HK, B-IU-210-HK, and C-210-HK, as listed in Table 1 and Fig. 2. Because all test specimens were symmetric, the left upper and lower slab is only drawn in Fig. 2. Specimen CTRL was a flat one-way slab and used as a control specimen to compare the one-way slabs with steps (Fig. 2(a)). Specimens N-210-HK and N-250-HK had 210 mm (8.3 in.) and 250 mm (9.8 in.) thicknesses of the step-in-slab, respectively, and no supplementary reinforcement was installed in the step. All the longitudinal reinforcement was anchored with 135-degree hooks within the step, as shown in Fig. 2(c). Specimens A-IU-210-HK and A-210-HK were reinforced by two supplementary bars of Type A (Fig. 2(f)), with one inverted U-bar additionally used in the step of A-IU-210-HK. For Specimen B-IU-210-HK, both Type B reinforcement and inverted U-bars were employed in the step. Specimen C-210-HK had supplementary reinforcement of Type C in the step with thickness of 210 mm (8.3 in.). For the first set of experiments, each slab longitudinal bar of the step was engaged with transverse reinforcement with a 135-degree hook in the step.

The plan of the second set of experiments was established based on the analysis of the results of the first experiment. The five specimens of the set were named IU-210-SLP, IU-400, A-IU-210, C-210, and C-210-LLS. Specimen IU-210-SLP had sloped steps with varying thickness from 210 to 390 mm (8.3 to 15.4 in.), as shown in Fig. 2(i). The inverted U-bar was only employed for the reinforcement of

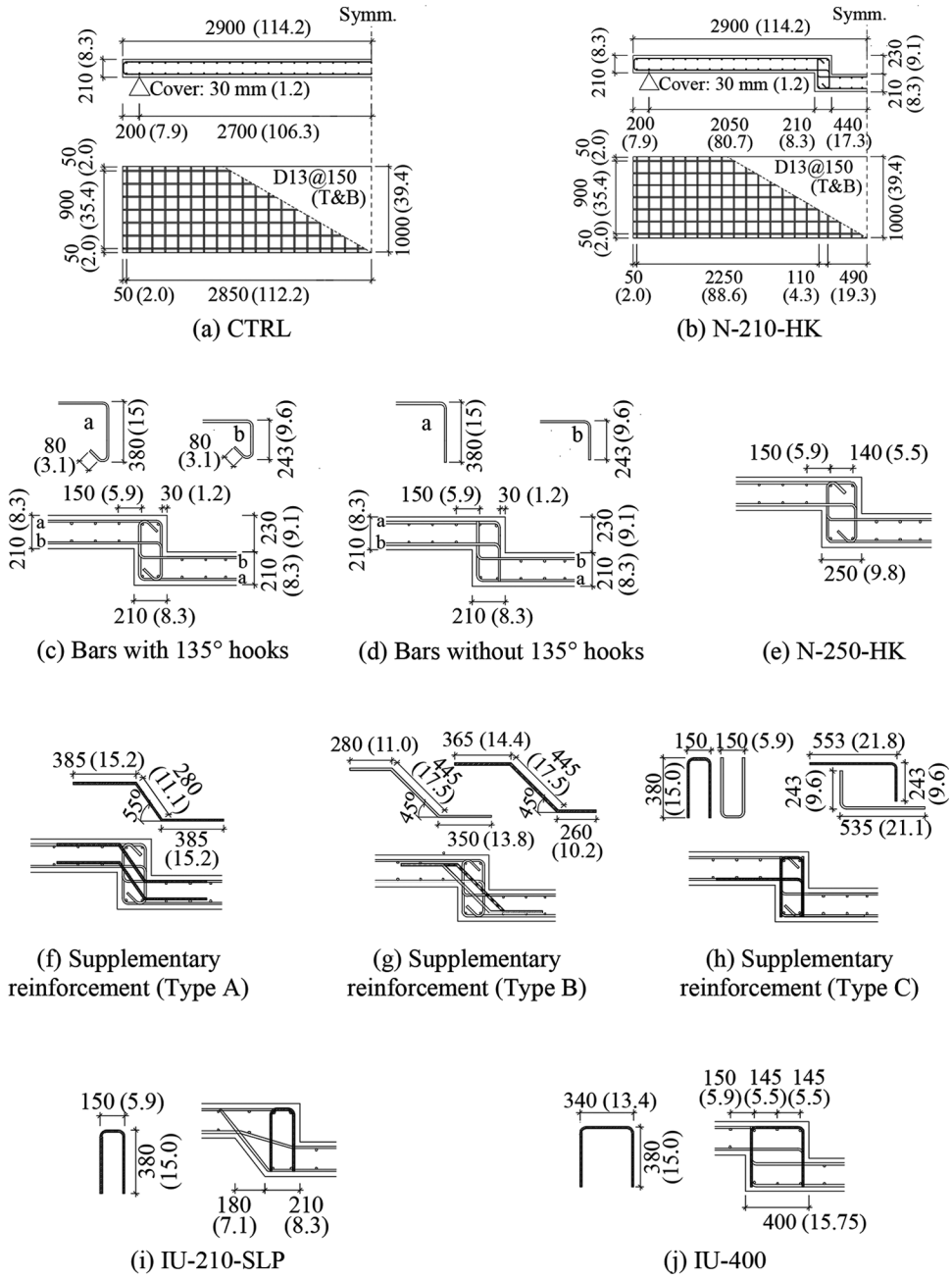

Fig. 2—Details of test specimens. (Note: Units are in mm [in.])

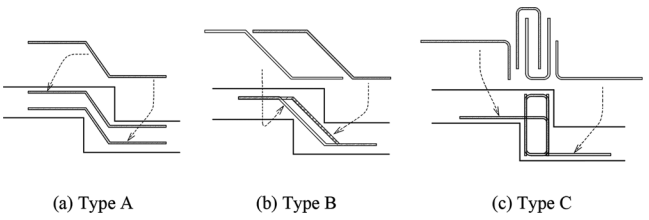

Fig. 3—Three types of supplementary reinforcement.

the step. The bottom main bar of the left upper slab, the top main bar of the lower slab, and the bottom main bar of the right upper slab were all continuous in one reinforcing bar. The bottom main bars of the lower slab were arranged along the inclined bottom surface, which had a horizontal length of 180 mm (7.1 in.). The end of the main reinforcing bar was not anchored with a hook of 135 degrees in the step. Specimen IU-400 had inverted U-bars and step thickness of 400 mm (15.8 in.), as displayed in Fig. 2(j). The supplementary reinforcement of Type A and inverted U-bar was used in A-IU-210 with a step thickness of 210 mm (8.3 in.), which is identical to A-IU-210-HK, except for the absence of the 135-degree hook in the step. Both C-210 and C-210-LLS specimens had Type C supplementary reinforcement and the same thickness (210 mm [8.3 in.]) of the step. Particularly, C-210-LLS had a long lower slab with 2700 mm (106.3 in.) length, which was 1610 mm (63.4 in.) longer than C-210.

Testing and instrumentation

Four-point loading was applied to the test specimens. Rollers were employed to support the test specimen and located at 200 mm (7.9 in.) from the end of the specimen such that the effective length of the specimen was 5400 mm

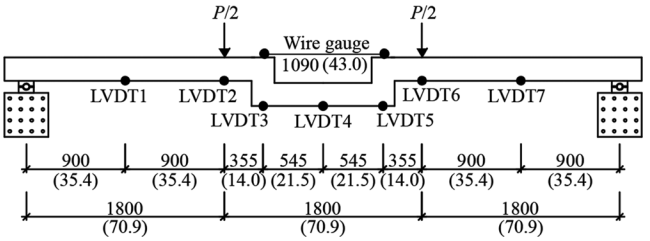

Fig. 4—Locations of line loads, wire gauge, and vertical LVDTs. (Note: Units are in mm [in.])

(212.6 in.) (Fig. 4). The distance between two loading points was 1800 mm (70.9 in.). The loads were applied to the entire width (1000 mm [39.4 in.]) of the one-way slab as line loads. Only for C-210-LLS with longer lower slab were the points of loads located inside the bottom slab of the step.

Seven linear variable differential transformers (LVDTs) were installed at the lower slab to measure the deflections of the specimen (Fig. 4). The deflection at each place was used to compute the rotation of the specimen between two points: θ_1 (LVDT1-LVDT2), θ_2 (LVDT3-LVDT4), θ_3 (LVDT4-LVDT5), and θ_4 (LVDT6-LVDT7). In other words, the rotation of the test specimens was estimated by the degree between the horizontal line and relative vertical displacement, and the moment transfer capacity can be evaluated through the values of θ_1 to θ_4.

A wire gauge was installed at the upper step level to measure the shortening due to rotation of the steps (refer to Fig. 4). In addition, strain gauges were installed to measure the strain on slab reinforcement, as depicted in Fig. 5(a). Additional gauges were located at the vital location of the reinforcing bar for the specimens with supplementary reinforcement (Fig. 5(b)). The surface of the specimens was painted white to identify the experimental progress and the occurrence of cracking, and grids of 50 x 50 mm^2 (1.97 x 1.97 in.^{2}) or 70 x 70 mm^2 (2.76 x 2.76 in.^{2}) were marked. The progress of cracking was also marked during the test.

EXPERIMENTAL RESULTS

Pattern of cracks and failure modes

Although the levels of cracks of one-way slabs with step were different, the pattern of cracks was similar to each other except for CTRL and IU-210-SLP. It was observed that cracks began at the exterior corner in the upper slab soffit, were concentrated in the upper part of the step, and propagated to the cover of the top slab, as shown in Fig. 6. Failure eventually occurred (refer to Fig. 6(h)). Due to self-weight of the actuator, approximately 30 to 60 mm (1.18 to 2.36 in.) length of cracks in the exterior corner was first detected (Fig. 6(a) and 6(b)) and the cracks in the bottom of the specimen were then observed in Fig. 6(c). The developed cracks in the bottom of the specimens did not progress significantly until the end of the experiment. The crack at the exterior corner propagated vertically and toward the interior corner, as demonstrated in Fig. 6(d). As the load increased, diagonal cracks developed from the exterior upper slab of the step to the interior lower slab (refer to Fig. 6(e)). In general, it was observed that the load rapidly dropped after such diagonal cracking except for in C-210-HK, C-210, and C-210-LLS.

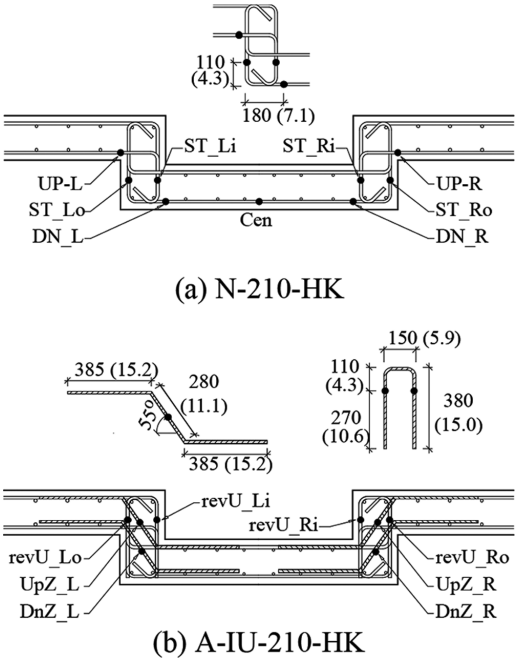

Fig. 5—Positions of strain gauges. (Note: Units are in mm [in.])

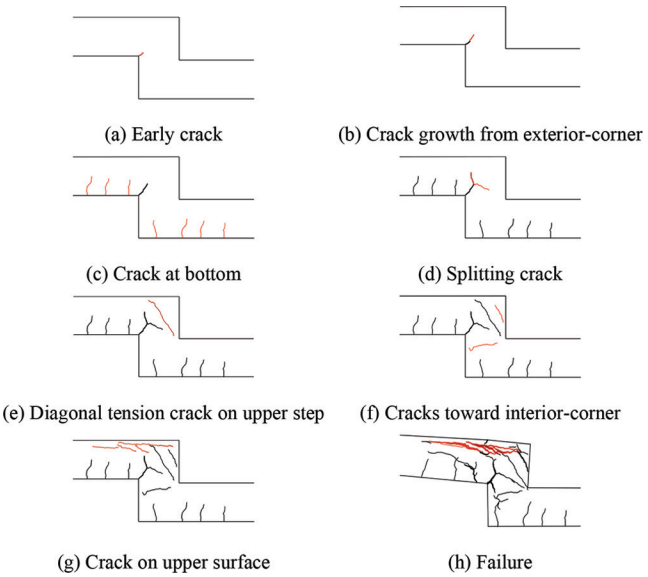

Fig. 6—Progression of cracks in B-IU-210-HK.

Also, the developed diagonal cracks propagated toward the interior corner and other cracks were initiated along the top cover of the upper slab, as displayed in Fig. 6(f) and 6(g), respectively. The experiment ended due to compressive failure at the interface of the upper slab and step. The final failure modes for all specimens are shown in Figure A1 of Appendix A. In the case of C-210-HK, crack width was minimized and crack spacing was relatively large. Even though IU-210-SLP did not show diagonal cracking in the upper step, it reached failure immediately after the early crack progressed.

Effect of shape of step

To examine the performance of different shapes of step, CTRL was compared to the other test specimens without

Table 2—Summary of test results

Specimens	L_c, mm	P_{cr}, kN	$P_{splitting}$, kN	$P_{diagonal}$, kN	P_u, kN	$\Delta_{initial}$, mm	$\Delta_{splitting}$, mm	$\Delta_{diagonal}$, mm	Δ_u, mm	$M_{max,test}$, kN·m	$M_{max,test}/M_{n,cal}$
CTRL	—	12.2	—	—	84.5	3.7	—	—	UNM	94	1.10
N-210-HK	16.5	7.5	8.4	22.5	27.0	2.4	6.9	60.3	142.0	45.1	0.57
N-250-HK	64.9	20.9	22.4	25.3	37.4	10.3	17.4	28.9	71.4	54.5	0.64
IU-210-SLP	18.2	19.3	25.7	None	50.6	11.2	20.8	None	117.5	66.9	0.79
IU-400	15.3	15.1	36.0	52.9	70.9	6.4	29.0	58.9	UNM	86.4	1.02
A-210-HK	64.8	24.2	28.1	31.7	46.8	23.2	29.4	42.4	140.0	62.5	0.74
A-IU-210-HK	87.9	23.2	31.6	34.3	61.1	16.8	28.1	36.8	111.9	75.4	0.89
A-IU-210	36.3	13.3	20.1	43.77	57.2	2.98	8.18	42.16	99.79	71.9	0.85
B-IU-210-HK	73.3	11.7	22.9	31.4	59.0	3.4	19.9	34.2	102.5	73.5	0.87
C-210-HK	69.1	11.6	23.5	35.3	78.6	2.4	16.4	32.9	UNM	91.1	1.08
C-210	61.8	10.7	23.4	39.6	74.9	2.0	14.0	34.5	145.5	87.8	1.04
C-210-LLS	19.0	9.5	23	48.3	78.9	1.9	17.1	45.8	UNM	87.8	1.08

Notes: L_c is length of corner crack; P_{cr} is load at initial cracking; $P_{splitting}$ is load at corner splitting crack; $P_{diagonal}$ is load at diagonal cracking in step; P_u is peak load; Δ_{cr} is displacement at initial cracking; Δ_u is displacement at failure; $\Delta_{diagonal}$ is displacement at diagonal cracking in step; Δ_u is displacement at peak load; UNM is unmeasured data; $M_{max,test}$ is experimentally measured maximum moment including moment due to self-weight; $M_{n,cal}$ is calculated nominal moment strength; 1 mm = 0.0394 in.; 1 kN = 224.8 lbf.

supplementary reinforcement. For N-210-HK, the ratio of maximum applied moment to nominal moment strength ($M_{max,test}/M_{n,cal}$) was 0.57 and the maximum rotation angle between two points of LVDT3 and LVDT4 (θ_2) was only approximately 0.001 radians or smaller, as shown in Table 2 and Fig. 7, respectively. Herein, $M_{max,test}$ is the measured maximum moment during the test plus the hand-calculated moment due to dead loads, and $M_{n,cal}$ is the calculated nominal moment strength as per ACI 318 (ACI Committee 318 2014). This was because early cracks were detected at the exterior corner and rapidly propagated with increased load. The maximum strain measured by the strain gauges at the midspan of N-210-HK was only 1314 μs, indicating that moment did not transfer through the step in the slab and the bending of the lower slab was very small. In the step, stiffness was rapidly reduced and the plastic hinge was formed as a result of the load transferred from the upper slab. The values of ($M_{max,test}/M_{n,cal}$) for N-250-HK, IU-210-SLP, and IU-400 were 0.69, 0.85, and 1.09, respectively.

Figure 8(a) depicts load-center displacement relationships for CTRL, N-210-HK, N-250-HK, IU-210-SLP, and IU-400. For CTRL, IU-400, C-210-HK and C-210LLS, the peak loads in Table 2 are different from those in Fig. 8 because the displacements were not measured until failure of the specimen due to the range of LVDT's stroke. In the early state of loading, N-250-HK, IU-210-SLP, and IU-400 exhibited smaller deflection at failure in comparison to CTRL. For N-250-HK, the secant stiffness at 20 kN (4.5 kip) was 2.27 kN/mm (12962.0 lb/in.), which was at the early stage of the experiment, and then the secant stiffness at three-fourths of the maximum load ($0.75P_{max}$) sharply dropped to 0.75 kN/mm (4282.6 lb/in.) (also refer to Table 3). In other words, the early stiffness of N-250-HK was larger than CTRL due to the thicker step, but it was difficult to obtain the maximum moment strength of CTRL at the ultimate state as the cracks progressed and stiffness dramatically decreased. Because inverted U-bars were installed in IU-210-SLP and IU-400,

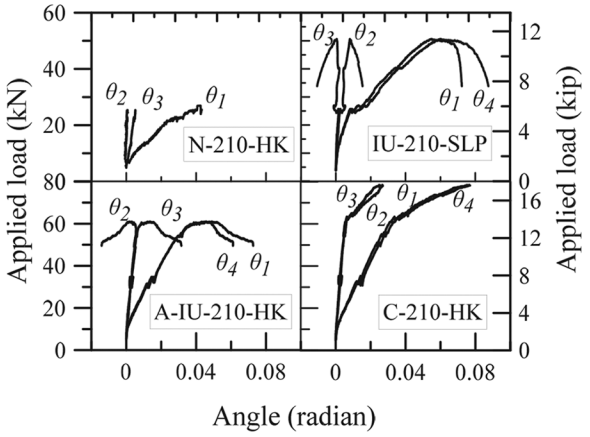

Fig. 7—Applied load-angle relations.

they obtained larger maximum moment strengths than N-250-HK. Based on the experimental results, it was found that it is not possible to have the same maximum moment strength as that of flat one-way slabs by simply increasing the thickness of the step.

Specimen IU-210-SLP had a 210 mm (8.3 in.) thick step and a 180 mm (7.1 in.) long transition slope on each side with respect to the midspan (refer to Fig. 2(g)). The maximum moment strength of IU-210-SLP was 66.9 kN-m (49342.9 lb-ft), which was only 71% of that of CTRL. The smaller deflection was observed until the load approached to 25 kN (5.6 kip), because IU-210-SLP exhibited larger stiffness than CTRL at the beginning (Fig. 8(a); also refer to Table 3). However, the stiffness rapidly decreased after a large crack occurred at the load of 25 kN (5.6 kip). The load-displacement curve in Fig. 8(a) demonstrates that the stiffness was dropped at 25 kN (5.6 kip). At this moment, the load applied to the upper slab was not transferred to the lower slab. The rotation angles between LVDT3 and LVDT4 points (θ_2) and between LVDT4 and LVDT5 points (θ_3) were also very small after the loading of 25 kN (5.6 kip) (Fig. 7).

Table 3—Secant stiffness at 20 kN and (3/4)P_{max}

Specimens	Δ_{20kN}, mm	$K_{sec,20kN}$, kN/mm	$\Delta_{(3/4)Pmax}$, mm	$K_{sec,(3/4)Pmax}$, kN/mm
CTRL	14.4	1.39	52.7	1.2
N-210-HK	46	0.43	47.7	0.43
N-250-HK	8.8	2.27	37.3	0.75
IU-210-SLP	12.3	1.63	65.1	0.58
IU-400	12	1.67	67	0.79
A-210-HK	19	1.05	67.9	0.52
A-IU-210-HK	12.8	1.56	55.7	0.82
A-IU-210	8.7	2.3	39.3	1.09
B-IU-210-HK	15.3	1.31	58.2	0.76
C-210-HK	11.6	1.72	68.9	0.86
C-210	9.7	2.06	67.5	0.83
C-210-LLS	14.2	1.41	59.7	0.94

Notes: Δ_{20kN} is midspan deflection at 20 kN; $K_{sec,20kN}$ is secant stiffness at 20 kN; $\Delta_{(3/4)Pmax}$ is midspan deflection at (3/4)P_{max}; $K_{sec,(3/4)Pmax}$ is secant stiffness at (3/4)P_{max}; 1 mm = 0.0394 in.; 1 kN = 0.225 kip.

Effect of supplementary reinforcement in step

Three specimens with steps and Type C supplementary reinforcement, such as C-210-HK, C-210, and C-210-LLS, had almost the same maximum moment as CTRL, as shown in Fig. 8(b). The ($M_{max,test}/M_{n,cal}$) values for these specimens were larger than 1, which represents over 100% of nominal moment strength (Table 2). The measured maximum moment of the three specimens are smaller than that of CTRL only by 6.7% on average. The supplementary reinforcement of Type C was very effective in suppressing the reduction of stiffness due to early cracking in the step and the reduction of the moment transfer capacity.

The maximum moments of A-IU-210-HK, B-IU-210-HK, and C-210-HK were measured to be 73.5, 75.4, and 91.1 kN-m (54,210.8, 55,612.2, and 67,191.9 lb-ft), respectively. Although all these specimens were installed with supplementary reinforcing bars, the flexural performance of the specimen reinforced with a combination of a U-bar, an inverted U-bar, an inverted L-bar, and an L-bar per each location (Fig. 3(c)) was better than those with one inverted U-bar and inclined bars (Fig. 3(a) and 3(b)). The moment value of C-210-HK was almost the same as CTRL at approximately 115 mm (4.5 in.) displacement. The Type A and B reinforcement did not perform well enough to achieve the full moment transfer capacity because the upper inclined bar was subjected to compressive force rather than tensile force.

The performance of an inverted U-bar is assessed by comparing the experimental results of A-210-HK and A-IU-210-HK. The maximum moment strengths of A-210-HK and A-IU-210-HK were 62.5 and 75.4 kN-m (46,097.6 and 55,612.2 lb-ft), respectively. It is considered that the difference between the maximum moment value results from the presence of the inverted U-bar that controls the cracking of the upper step. The maximum bar strain of the revU_Lo series (refer to Fig. 5(b)) at the point of the interface between the left inverted U-bar and upper slab was 6432 μs. The specimens without inverted U-bars (N-210-HK and A-210-HK) had their

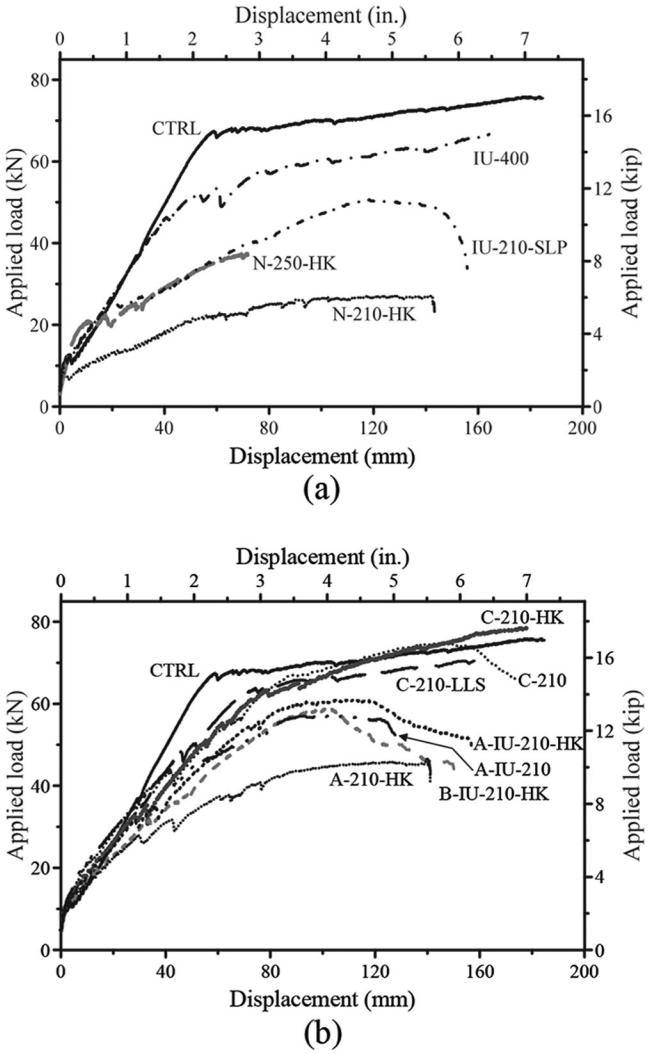

Fig. 8—Applied load-displacement relationship.

early stiffness greatly reduced (also refer to Table 3). This result indicates that the inverted U-bar withstood a great force and controlled diagonal cracking reasonably well.

Specimens C-210-HK and C-210 were prepared in the same condition except for the end finishing of the tail of main slab hooked bars in the step, which is similar to a seismic hook (Fig. 2(b)). Specimen C-210-HK had the 135-degree hook at the end of each main bar that engaged a transverse slab reinforcing bar, whereas C-210 had a straight end. The $M_{max,test}$ of C-210-HK was 91.1 kN-m (67,191.9 lb-ft), which was larger than that (87.8 kN-m [64,758 lb-ft]) of C-210. Figure 8(b) shows that the load-displacement behaviors of the two specimens were very similar. The final measured moment for CTRL was larger than C-210-HK according to the load cell data. Again, it is noted that displacement data were not obtained beyond the displacement of 178 mm (7 in.) due to the LVDT stroke limitation, but load data were kept to be measured. The concrete compressive strengths of C-210-HK and C-210 were 30.0 and 23.1 MPa (4.4 and 3.4 ksi), respectively, indicating that difference in the compressive strength might have influenced the $M_{max,test}$. Based on the comparison, it is concluded that the end finishing with a 135-degree hook at the end of the tail of slab hooked bars is not required.

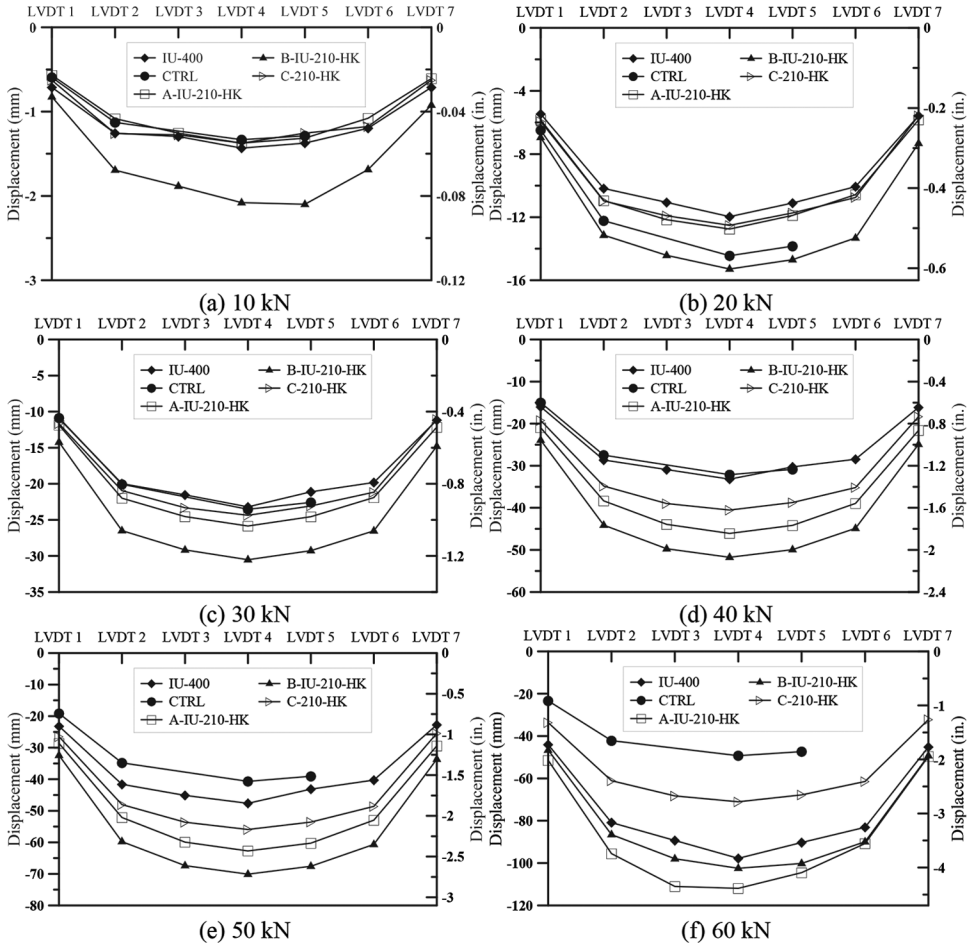

Fig. 9—Displacement distributions by load stages.

Figure 9 shows displacement diagrams at each loading stage for five specimens: CTRL, IU-400, A-IU-210-HK, B-IU-210-HK, and C-210-HK. At loading stages of 10 and 30 kN (2.25 and 6.75 kip), their displacement pattern was similar to each other except for B-IU-210-HK. The displacement of B-IU-210-HK was the largest, and CTRL had the second largest at 20 kN (4.5 kip) loading, as shown in Fig. 9(b). The displacements of CTRL and IU-400 were very close to each other at the loading stage of 40 kN (9.0 kip), while B-IU-210-HK had the larger displacement than that of A-IU-210-HK and C-210-HK, as exhibited in Fig. 9(d). In the case of IU-400, the displacement dropped sharply between 50 and 60 kN (11.2 and 13.5 kip). Because C-210-HK had the smallest displacement at 60 kN (13.5 kip), it was found that the supplementary reinforcement of Type C in step was the most effective. Consistent displacement data would ensure more reliability and accuracy of the measurement.

Specimens A-IU-210-HK and A-IU-210 were reinforced with Type A reinforcement and an inverted U-bar per each location. Specimen A-IU-210-HK was reinforced by inclined SD500 D13 bars (f_y = 500 MPa [72.5 ksi] and diameter = 13 mm [0.5 in.]), while A-IU-210 was reinforced by inclined SD600 D16 bars (f_y = 600 MPa [87 ksi] and diameter = 16 mm [0.625 in.]). The $M_{max,test}$ values of the specimens were 75.4 and 71.9 kN-m (55,612 and 53,031 lb-ft), respectively. This indicates that the increase in the amount and yield strength of the inclined bars did not significantly influence the flexural moment of the slab with step. The compressive concrete strengths of A-IU-210-HK and A-IU-210 were 29.8 and 23.1 MPa (4.3 and 3.4 ksi), respectively. Figures 10(a) and 10(b) show that the maximum strain values of inclined bars did not reach the yield strain and that the inclined bar did not withstand much force. Specifically, the strain gauges (UpZ_L series, UpZ_R series) installed at the upper inclined bar monitored compressive strains in the same direction as that of diagonal tensile cracking. On the contrary, the strain gauges (DnZ_L series, DnZ_R series) located at the lower inclined bar had tensile strains. The diagonal crack occurred only at the upper part of the steps (refer to Fig. 6).

The step of C-210-LLS was installed between the loading points, which were located outside steps, so that substantial shear force was applied along with flexural moment on the step. Comparing the strain of the main bottom slab bar, the strain gauge (Up_L) at the interface of left upper slab and step and the strain gauge (Dn_L) at the interface of left lower slab and step had quite small values of 1883 and 1509 με, respectively. Conversely, the strain gauge (C) attached on the bottom bar at the center of the lower slab exhibited 40,799 με, as shown in Fig. 10(c). The strain gauge data demonstrate that the moment transfer capacity of the step was sufficient to develop the full plasticity of the lower slab.

Figure 11 illustrates relations between the applied load and bar strain. The detailed location of strain gauges is shown in Fig. 5. Specimen CTRL was used as a reference, of which

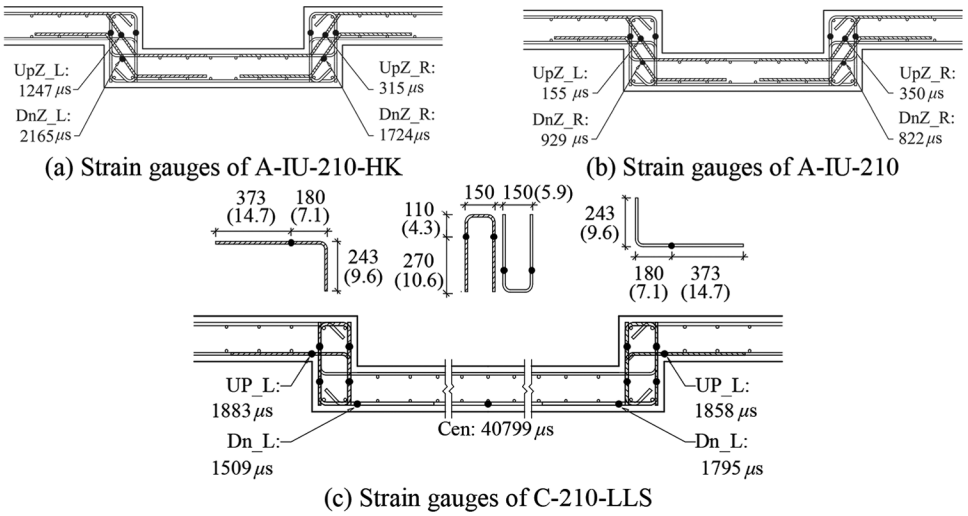

Fig. 10—Maximum strains of bars.

the strains monotonically increased and exceeded the yield strain with increased load. For most of the specimens except for ones reinforced by Type C reinforcement, the strains of UP_L and UP_R exceeded 2000 μs, but those of DN_L and DN_R were smaller than 2000 μs. This confirms that the bending moment was not appropriately transferred to lower slab. In Fig. 11(d) and 11(e), the strains of DN_L and DN_R for IU-210-SLP and IU-400 were suddenly dropped at the load of 50 and 70 kN (11.2 and 15.7 kip), respectively, because diagonal cracks were initiated at these moment values. Figures 11(f), 11(g), and 11(h) show the load-bar strain curves for the slabs with step reinforced by Type C reinforcement. The strains of DN_L and DN_R were close to 2000 μs, indicating that the Type C reinforcement was effective in controlling the diagonal cracks in steps.

DESIGN OF REINFORCEMENT IN STEP OF SLAB

The experimental results indicate that: 1) the specimen with the step reinforced with Type C reinforcement had equivalent flexural strength of CTRL; 2) L-bars and inverted L-bars, which were placed parallel to the main slab bar, resulted in the yield of the main bar away from the step; and 3) inverted U-bars and U-bars were effective in controlling the damage to the step. Tensile cracking due to diagonal tensile force in the upper step resulted in early damage and failure, inducing significant strains in the bottom bars adjacent to the step without a combination of an L-bar, an inverted L-bar, a U-bar, and an inverted U-bar. As a result of the diagonal tension, ductility of the joint was not ensured. For the design to attain flexural strength and ductility similar to those of flat slab, it is necessary that the yield of slab bottom bars anchored in steps be prevented and adequate bonding capacity be secured. This can be achieved by adding L-bars and inverted L-bars in step, which was confirmed by the experimental results of C-210-HK, C-210, and C-210-LLS. The diagonal cracks in the upper step can be controlled by adding an inverted U-bar (Fig. 12(a)). Although the lower step is subjected to diagonal compressive stress under gravity loading (Fig. 12(b), the addition of a U-bar is necessary to have sufficient anchorage capacity of the vertical legs of the inverted U-bar.

The slab bars at the top and bottom of upper and lower slabs are anchored in step with a 90-degree hook. It is advisable that the hook tails of top and bottom bars be extended up to the bottom of the lower slab (or top of the upper slab) minus the minimum concrete cover (Fig. 13). Also, it is recommended that four transverse reinforcing bars be engaged with the main slab bars at the corners of the step, including the inner bearing location of the hook.

On basis of the yield of main slab bars and the force equilibrium shown in Fig. 12, the force exerting on the step is determined and the quantity of inverted U-bars is computed as expressed in Eq. (1).

$$A_s f_y \le A_{s\_iU} f_{y\_iU} \tag{1}$$

where A_s is the total cross area of slab bottom reinforcement of upper slab per unit width (mm^2/mm); A_{s_iU} is the total cross area of vertical legs of inverted U-bars per unit width (mm^2/mm); f_y is the specified yield strength of slab bottom reinforcement of upper slab (MPa); and f_{y_iU} is the specified yield strength of inverted U-bars (MPa). The quantity of U-bars is set to be the same as that of inverted U-bars. This is because the functions of the inverted U-bar and U-bar are switched when negative moment is exerted (for example, under seismic actions). The lapped length (l_{l_iU} or l_{l_U} in Fig. 14(a) and 14(b)) for the provided inverted U-bars or U-bars was 302 mm (11.9 in.), while the development length l_d required for a deformed bar was determined to be 386 mm (15.2 in.) according to Eq. (25.4.2.3a) of ACI 318-14. Although the lapped length for inverted U-bars and U-bars is less than $1.3l_d$, the height h and width w of the inverted U-bar and U-bar are recommended to be determined based on the size of step, the minimum concrete cover, and the determined quantity using Eq. (1) (refer to Fig. 14(a) and 14(b)).

If steps are subjected to positive moment only, the bottom bars of upper and lower slabs should be reinforced (Fig. 14(c) and 14(d)). The strain gauge data indicated that the specimens with L-bars and inverted L-bars resulted in yielding of the main slab bars far away from the steps and obtained almost the same flexural strength as that of flat slab. The quantity of the L-bar or inverted L-bar can be set equal to that of the

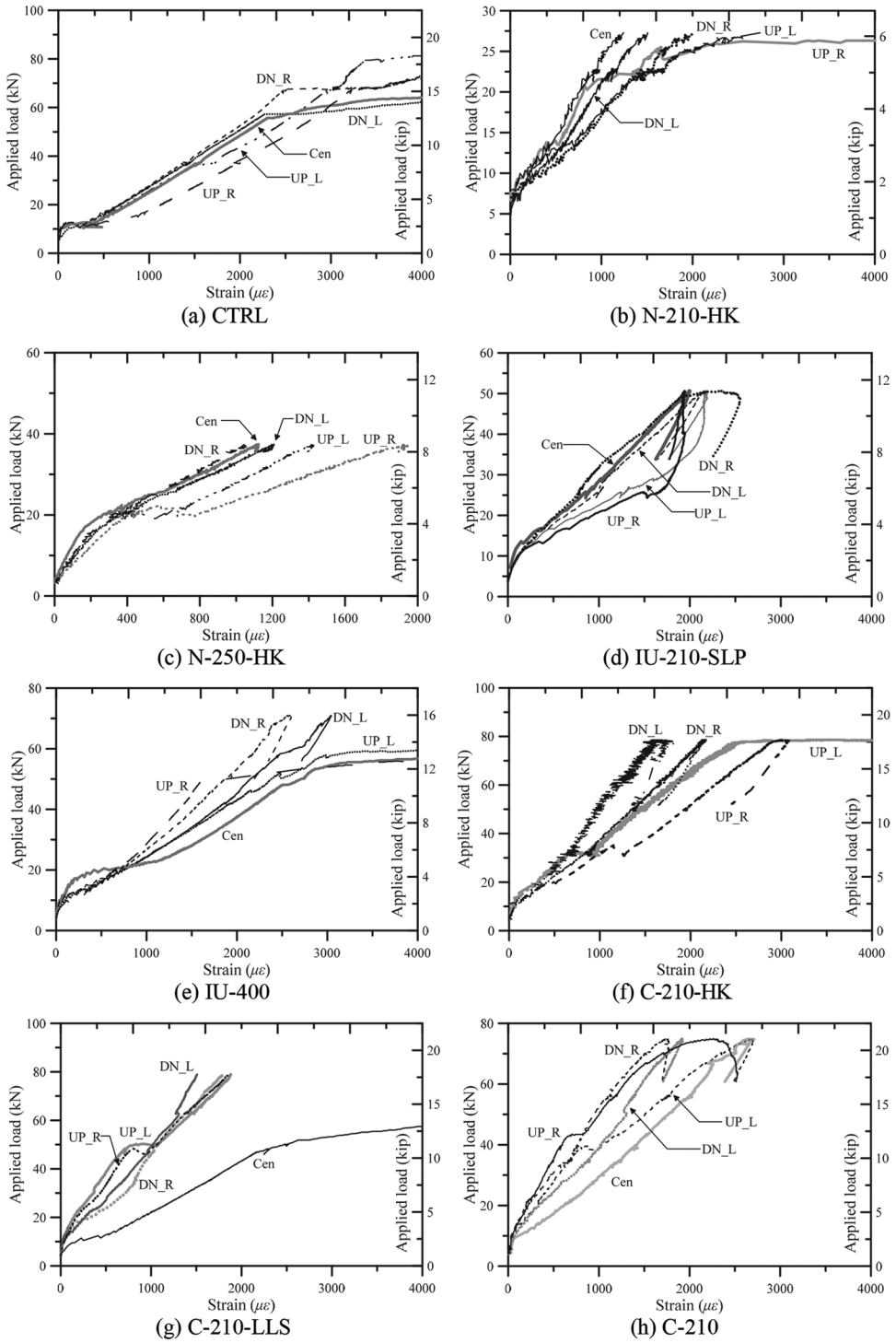

Fig. 11—Applied load-bar strain relationship.

main slab reinforcing bar at that location, because it is easier to obtain the same size of reinforcing bars at its job site, and the same concrete covers can be applied to both longitudinal and transverse slab reinforcement. The development length (l_d; refer to Fig. 14) for the straight portion of L-bars or inverted L-bars from the interface between lower or upper slab and step is computed in accordance with ACI 318-14. This was satisfied by applying Eq. (25.4.2.3a) of ACI 318-14 in the experiment; however, the development length (l_{dh_iL} or l_{dh_L} in Fig. 14(c) and 14(d)) for the hook of inverted L-bars or L-bars was 180 mm (7.1 in.)—smaller than the required developed length l_{dh} of 318 mm (12.5 in.) as per Section 25.4.3 of ACI 318-14. The tail length (l_{ext_iL} or l_{ext_L} in Fig. 14(c) and 14(d)) of the hook was 191 mm (7.5 in.), which was also greater than 12 of the bar diameter (d_b) (156 mm [6.1 in.]). In any case, the tail of the 90-degree hook of L-bars and inverted L-bars should be located at the far face from the potential critical section in the step minus the minimum concrete cover. If the step is subjected to both positive and negative moments, the top bars of upper and lower slabs should also be reinforced (Fig. 14(e) and 14(f)).

It is desirable to meet the development length standards for supplementary reinforcement, but typically not possible given the dimension of the step and size of main slab bars.

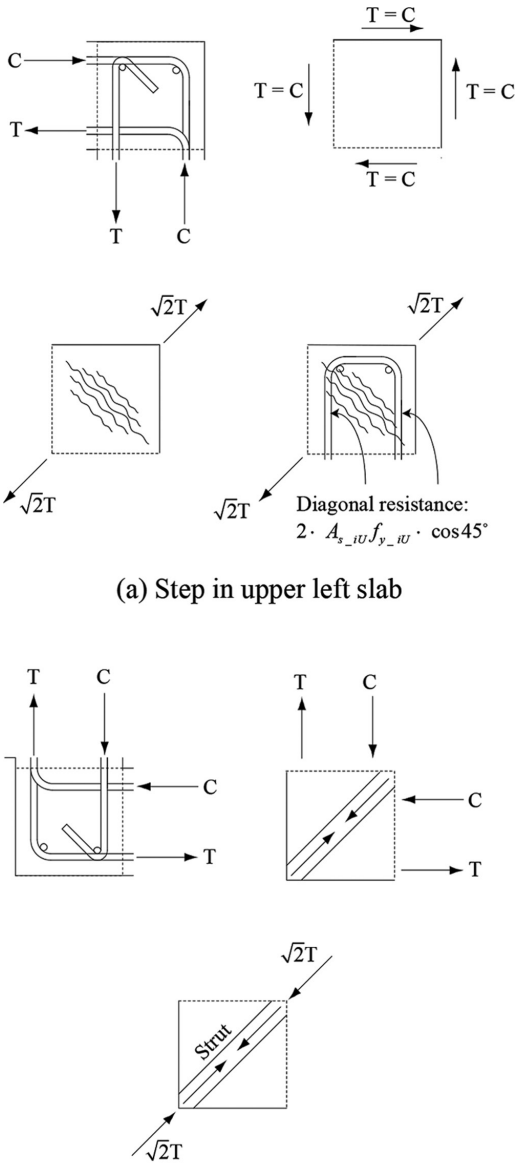

Fig. 12—Forces in step.

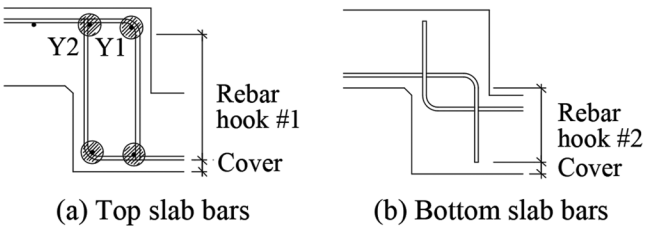

Fig. 13—Tail length of hooked bars in step.

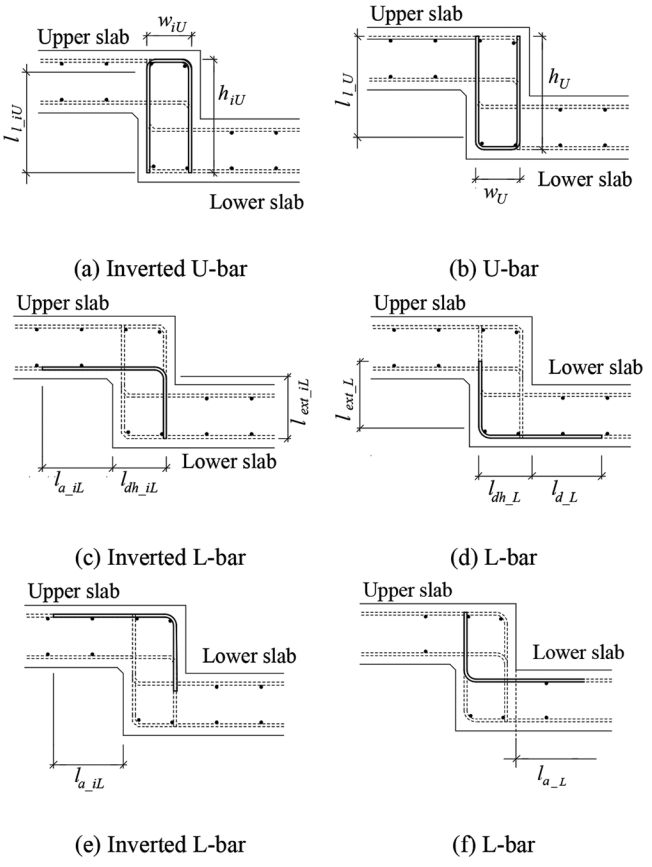

Fig. 14—Design of supplementary reinforcement in step.

Because there is also overlapping with main slab reinforcement, the development of supplementary reinforcement would be expected to be better than no overlap. Therefore, once the dimension of stepped slab and size of main bars in the upper and lower slabs are determined, it is recommended that the quantity of supplementary reinforcement in step is first chosen and the maximum size of supplementary reinforcement is then determined for design.

CONCLUSIONS

This study was conducted to evaluate the structural performance of one-way reinforced concrete slabs with step in terms of flexural strength, stiffness, deflection, and cracking. Reinforcement details in the step were proposed based on thorough investigation of experimental data. The experimental investigation results in the following conclusions:

1. The experimental results show that the stepped slab is too weak to maintain adequate flexural capacity of the slab. The maximum measured moment to nominal moment strength without additional reinforcement was only 0.57. Cracking in and around the step rapidly propagated, and the moment transfer capacity to the slab was degraded soon after substantial diagonal cracks were developed. However, it was found that the slab with step properly detailed by using a group of supplementary reinforcing bars had a capacity to restrain the yield of slab reinforcement adjacent to the step and to transfer flexural moment.

2. The early secant stiffness of the slab with step was larger than that of the one-way slab without step according to the supplementary reinforcement and detailing in step. Particularly, it was observed that the test specimens reinforced by inverted U-bars had proper secant stiffness at an early stage by controlling the diagonal cracks. However, as these diagonal cracks were more developed and propagated, its secant stiffness was significantly reduced compared to that of the one-way slab.

3. The details of the following reinforcement were recommended: 1) supplementary reinforcement of L-bars and inverted L-bars should be placed at the slab bottom if it is

subjected to positive moment only, while if both positive and negative moments take place, L-bars and inverted L-bars should be placed at the slab top; 2) inverted U-bars should be placed to control diagonal cracks in the step and the same quantity of U-bars is provided in the step to promote the anchorage capacity of the vertical legs of inverted U-bars (or vice versa for moment reversal); 3) the quantity of supplementary reinforcement in the step should be determined by the quantity of the main slab reinforcement; and 4) the development and lapped length of supplementary reinforcement should be determined from the given dimension of the step of slab and size of main slab bars first, and then by the ACI 318 Code.

AUTHOR BIOS

Thomas H.-K. Kang, *FACI, is an Associate Professor at Seoul National University, Seoul, Korea. He is a member of ACI Committee 369, Seismic Repair and Rehabilitation; and Joint ACI-ASCE Committees 335, Composite and Hybrid Structures; 352, Joints and Connections in Monolithic Concrete Structures; and 423, Prestressed Concrete, and Joint ACI-ASME Committee 359, Concrete Containments. He received the 2009 ACI Wason Medal for Most Meritorious Paper. His research interests include the design and behavior of reinforced and prestressed concrete structures.*

ACI member **Sanghee Kim** *is a PhD Student at Seoul National University. He received his BS from Jeonbuk National University, Jeonju, South Korea, and his MS from Seoul National University. His research interests include the structural behavior and impact resistance of reinforced concrete and steel fiber-reinforced concrete structures.*

Seongwon Hong *is an Assistant Professor at Korea National University of Transportation, Chungju, South Korea. He received his BS from Chung-Ang University, Seoul, Korea; his MS from Stanford University, Stanford, CA; and his PhD from the University of California, Los Angeles (UCLA), Los Angeles, CA. His research interests include the behavior of reinforced concrete structures, and computational and damage-healing mechanics of concrete and heterogeneous composites.*

Geon-Ho Hong *is a Professor at Hoseo University, Asan, Korea. He received his BS, MS, and PhD from Seoul National University. His research interests include the behavior of reinforced concrete structures, and concrete materials and concrete mixture design.*

ACI member **Hong-Gun Park** *is a Professor at Seoul National University. He received his his BS and MS in architectural engineering from Seoul National University and his PhD in civil engineering from the University of Texas at Austin, Austin, TX. His research interests include inelastic analysis and the seismic design of reinforced concrete structures.*

ACKNOWLEDGMENTS

The work was supported by Land & Housing Corporation grant and National Research Foundation of Korea (NRF) Grant (No. 2015-001535). The views expressed are those of the authors, and do not necessarily represent those of the sponsors.

REFERENCES

ACI Committee 318, 2014, "Building Code Requirements for Structural Concrete (ACI 318-14) and Commentary (ACI 318R-14)," American Concrete Institute, Farmington Hills, MI, 519 pp.

American Concrete Institute, 2012, "Detailing Corner: Steps in Beams," *Concrete International*, V. 34, No. 6, June, pp. 41-44.

Architectural Institute of Korea, 2009, "Korean Building Code and Commentary 2009," Kimoondang Publishing Co., 1040 pp. (in Korean)

Han, S. W.; Kee, S.-H.; Park, Y.-M.; Lee, L.-H.; and Kang, T. H.-K., 2006, "Hysteretic Behavior of Exterior Post-Tensioned Flat Plate Connections," *Engineering Structures*, V. 28, No. 14, pp. 1983-1996. doi: 10.1016/j.engstruct.2006.03.029

Hueste, M. B. D., and Wight, J. K., 1999, "Nonlinear Punching Shear Failure Model for Interior Slab-Column Connections," *Journal of Structural Engineering*, ASCE, V. 125, No. 9, pp. 997-1008. doi: 10.1061/(ASCE)0733-9445(1999)125:9(997)

Kang, T. H.-K., and Wallace, J. W., 2005, "Dynamic Responses of Flat Plate Systems with Shear Reinforcement," *ACI Structural Journal*, V. 102, No. 5, Sept.-Oct., pp. 763-773.

Kang, T. H.-K.; Wallace, J. W.; and Elwood, K. J., 2009, "Nonlinear Modeling of Flat-Plate Systems," *Journal of Structural Engineering*, ASCE, V. 135, No. 2, pp. 147-158. doi: 10.1061/(ASCE)0733-9445(2009)135:2(147)

Lee, J. D.; Yoon, J. K.; and Kang, T. H.-K., 2016, "Combined Half Precast Concrete Slab and Post-Tensioned Slab Topping System for Basement Parking Structures," *Journal of Structural Integrity and Maintenance*, V. 1, No. 1, pp. 1-9. doi: 10.1080/24705314.2016.1153281

Moehle, J. P., 1996, "Seismic Design Considerations for Flat-Plate Construction," *Mete A. Sozen Symposium: A Tribute from His Students*, SP-162, J. K. Wight and M. E. Kreger, eds., American Concrete Institute, Farmington Hills, MI, 460 pp.

Rha, C.; Kang, T. H.-K.; Shin, M.; and Yoon, J. B., 2014, "Gravity and Lateral Load-Carrying Capacities of Reinforced Concrete Flat Plate Systems," *ACI Structural Journal*, V. 111, No. 4, July-Aug., pp. 753-764. doi: 10.14359/51686731

Robertson, I. N.; Kawai, T.; Lee, J.; and Enomoto, B., 2002, "Cyclic Testing of Slab-Column Connections with Shear Reinforcement," *ACI Structural Journal*, V. 99, No. 5, Sept.-Oct., pp. 605-613.

APPENDIX

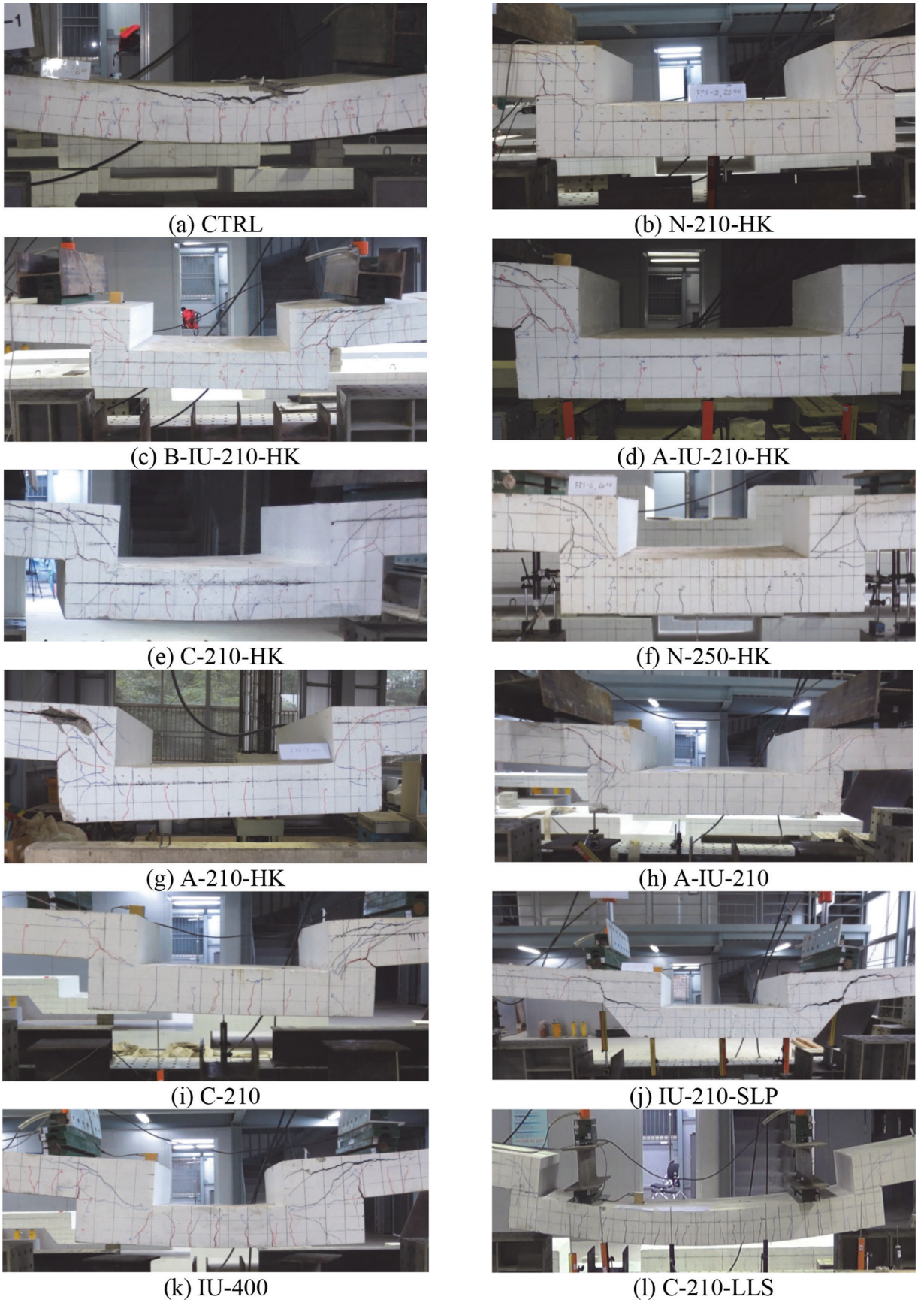

Fig. A1—Features of failure for test specimens.